photonics

MDPI

Communication

Temperature Monitoring in PIC Surface

Sushma Pandey [1,2,*], Antonio Teixeira [1,2] and Mario Lima [1,2]

[1] Instituto de Telecomunicações (IT), 1049-001 Lisbon, Portugal
[2] Department of Electronics, Telecommunications, and Informatics (DETI), University of Aveiro, 3810-193 Aveiro, Portugal
* Correspondence: pandey@ua.pt or pandey@av.it.pt

Abstract: In this work we present the extended work of the previously proposed scheme for in-PIC temperature monitoring. This can be used in any photonic integrated circuitry platform, allowing simplified temperature monitoring and improved independence of the interrogating laser wavelength. Theoretically, power sensitivity was observed to be 0.77 dB/°C and 0.98 dB/°C for common mode and differential mode, respectively. The experimentally noted sensitivity of common mode and differential mode are 1.45 dB/°C and 0.8 dB/°C, respectively, at 1524 nm. The scheme allows the monitoring of the average temperature on the surface of the chip, which results from the global effect that affects both gratings (common mode) and the monitoring of the difference in temperature between gratings (differential mode).

Keywords: photonics integrated circuit; grating; temperature monitoring

1. Introduction

Bragg gratings are waveguides in which the effective refractive index varies periodically, inducing a resonance in the mode traveling through it, which will result in the reflection of a band centered on a specific wavelength that is related to periodicity. The easiest way to vary the refractive index of a Bragg waveguide is by altering its geometry, determining the grating strength, and the Bragg wavelength (i.e., the center wavelength of the grating) [1].

Photonic integrated circuits (PICs), similar to integrated electronics, are the next-level solution for photonic complexity and are important in handling photonic complexity and availability. Permitting the integration of many components onto one chip provides a concept such as a photonic system-on-chip. PICs have a number of key advantages compared with conventional bulk free-space photonics, such as shorter optical path lengths between devices and the availability of high-speed optoelectronic components with bandwidth greater than 40 GHz [2]. Yet another major problem in PICs is a trade-off between chip shrinking and a heat dissipation problem in active parts, due to miniaturization and high component density. However, these highly active components also produce heat that may deteriorate the performance of temperature-sensitive chip components and make controlling the safe operation more complicated. Indium phosphide (InP) is the most promising material chosen to fabricate an integration platform that integrates both active and passive devices monolithically at the same time [3]. Thermal, RF, and optical crosstalk also need to be mitigated in a scalable PIC [4,5]. Although RF and optical crosstalk is an old and widely known problem occurring in electronic ICs, which can be avoided or at least reduced through well-established design rules, optical crosstalk can also be handled via foundry DRCs (design rule checks) that participate in automated detection of major flaws

check for updates

Received: 19 November 2024
Revised: 21 December 2024
Accepted: 3 January 2025
Published: 9 January 2025

Citation: Pandey, S.; Teixeira, A.; Lima, M. Temperature Monitoring in PIC Surface. *Photonics* **2025**, *12*, 54. https://doi.org/10.3390/photonics12010054

during the design phase. The situation is more complicated regarding thermal crosstalk, as active components, such as lasers, are very sensitive to temperature and will have detrimental interaction with other components on the chip [6]. As such, one of the keys to a well-performing PIC is its thermal management. Global thermal stabilization of the PIC in a photonic device is usually performed with a thermoelectric cooler (TEC), which allows extending the operational temperature of the components in the chip and helps prevent heat damage in the devices [7]. To close the temperature control loop, a thermistor is normally used, placed close to the chip. However, the TEC controls the chip temperature globally, but the temperature at the chip surface varies drastically with any heat source [6,7]. A state-of-the-art approach involves integrating Bragg grating sensors into photonic integrated circuits (PICs) to monitor temperature fluctuations, which are common in optical interconnect applications. The wavelength shift in Bragg gratings caused by temperature changes serves as a precise and reliable method for detecting and compensating for such fluctuations [8].

Research [5–7] has identified the presence of thermal crosstalk between neighboring components even when thermal control is active, due to the distance between the sensor (the thermistor) and the component generating the heat. The work we present has two methods named common mode (average displacement of the grating caused by heating) and differential mode (differential displacement caused by heating). A simplified schematic of the common mode is shown in Figure 1, illustrating the electrical connection of a photonic integrated circuit (PIC) that includes several active or heat-controlled building blocks (BB). The block diagram for the differential mode was previously presented in our earlier work [9], where a laser generates heat that affects the entire PIC. Most studies focus on either enhancing the thermal flow or improving the sensitivity of the sensor [7].

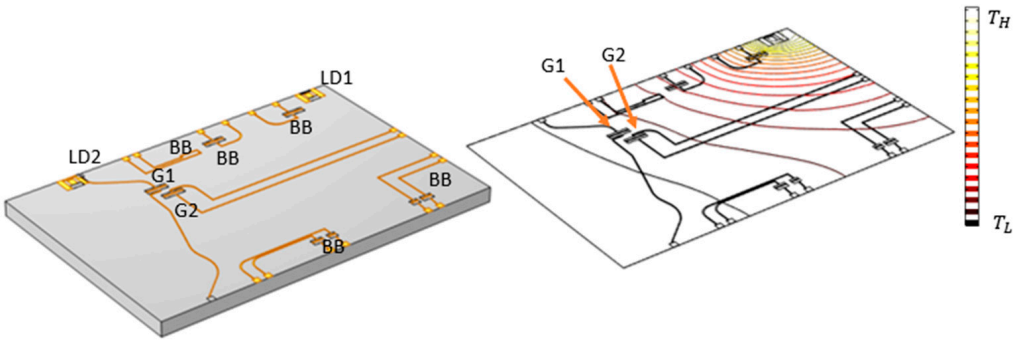

(**a**) (**b**)

Figure 1. (**a**) Example diagram showing electrical connection of a PIC comprising several active or heat-controlled building blocks (BB) (**b**) Contour of temperature over the surface of exemplary PIC when LD2 is on biased at high current (T_H: higher temperature; T_L: lower temperature).

In this study, we extend our previous research [9], which provided a theoretical analysis of the topic. This work introduces and defines a setup that leverages the conventional temperature dependence of gratings, enhancing it to ensure compatibility with variations in the interrogator laser wavelength. This technique is simple, and after calibration, it can provide both differential and absolute temperature on the photonic chip's surface [9]. This capability of having the differential temperature is the key strength of the method, whereas absolute temperature can also be achieved through conventional grating-based temperature sensors. This scheme is based on an interrogator laser, which in InP can be built in, or in the other platforms can be externally or hybrid like integrated, and a set of pairs of gratings designed in a very specific way such that their wavelengths are by design very close to each other.

2. Grating-Based Scheme

In Figure 2 it is the basis for the designed structure as well as the block diagram of the scheme. The design structure is like our previous work [9]. Where two modes were proposed theoretically: common mode and differential mode. The average displacement of the two gratings caused by the heating of an active device laser diode (LD in our case is DFB-L1) is called common mode. And the difference in the two displacements is termed as differential mode. These two modes allow us to have an estimation of the average temperature change and the effective local temperature.

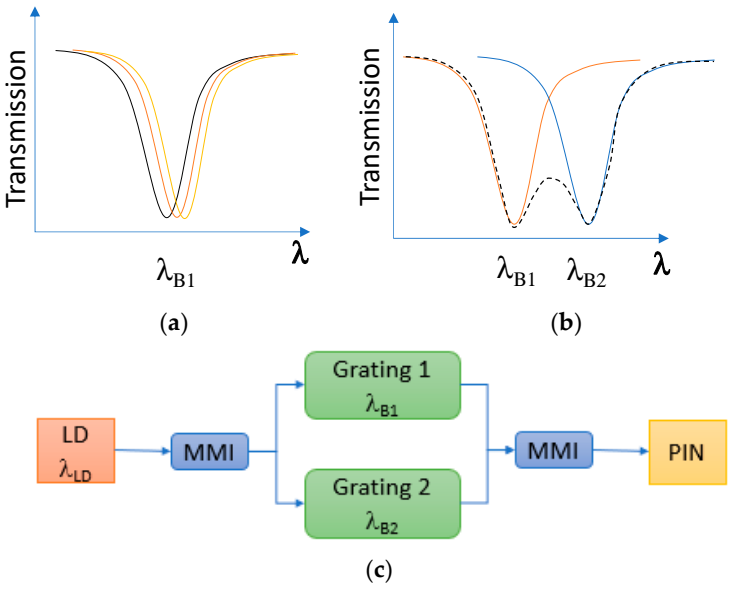

Figure 2. (**a**) Transmission spectrum of a grating with Bragg wavelength l_{B1} for different temperatures. (**b**) Two Bragg gratings with Bragg wavelengths λ_{B1} and λ_{B2}. (**c**) Block diagram of the scheme. LD—laser diode with wavelength $\lambda_{LD} \in [\lambda_{B1}: \lambda_{B2}]$; MMI—multimode interferometer 1:2 splitter/combiner configuration; PIN—Photodiode.

The scheme allows for monitoring the average temperature, which results from the global effect that affects both gratings (common mode). For an example, if T_0 is the ambient temperature, then the average operating temperature could be considered as $T_0 + \Delta T_{cm}$ for the common mode operation, where ΔT_{cm} is the common mode temperature. With turning ON the LD, the average temperature of grating, which is dependent on the position/location from LD represented here as G_x, so the new temperature when LD is ON can be represented as $T_0 + \Delta T_{cm} + \Delta T_{LD \to Gx}$. The central wavelength of the grating is dependent on the temperature locally and is represented as $\lambda_{G1}(T)$ and $\lambda_{G2}(T)$. Thus, with everything OFF, we obtain $\lambda_{G1}(T_0)$ and $\lambda_{G2}(T_0)$. If we switch all other devices, the new λ_{G1} $(T_0 + \Delta T_{cm})$ and λ_{G2} $(T_0 + \Delta T_{cm})$. At last, by removing T_0, we have ΔT_{cm}, i.e., the common mode component.

In the case of differential mode, the effects of temperature on the Bragg wavelength of G1 and the combination of the gratings, i.e., G1 & G2 are modeled and studied for monitoring the differential temperature at PIC. One of the gratings suffers a negligible wavelength shift because it is far from the heat source. In our case, this grating is G2. For example, if we switch ON the LD, we will have $\Delta T_{LD \to G1}$ and $\Delta T_{LD \to G2}$ for G1 and G2, respectively. Now, assuming that G1 is present close to LD, then $\Delta T_{LD \to G1} >> \Delta T_{LD \to G2}$. We obtain $\Delta T_{LD \to G1}$ as the local temperature near G1 (operation in differential mode).

Each of the gratings presents a wavelength dependence on the temperature as depicted in Figure 2a. The profile is shifting with temperature. Both gratings have similar behavior

since they are designed to be very similar and on the same substrate. In the arrangement, the two Bragg gratings with Bragg wavelengths λ_{B1} (1522 nm) and λ_{B2} (1529 nm) of length 300 µm are designed in such a way that the right slope of the transmission spectrum of the lower Bragg wavelength overlaps with the left slope of the transmission spectrum of the higher wavelength grating (as shown in Figure 2b). This design allows the overlap spectrum to behave in a way that the full shape can be controlled by controlling each Bragg wavelength design or temperature. The part in between the grating's transmission functions will change with the temperature and present a wider bandwidth than a simple single grating structure, making the structure much more resilient to the interrogator laser wavelength variations, making this method very insensitive to the offset temperature of the chip or the laser fabrication tolerances. The gratings are placed very close to each other to be similarly affected by the temperature of the heat-generating component. The full structure may be very small since the gratings are almost unidimensional from the design point of view. In the Heinrich Hertz Institute (HHI) InP platform, the LD's present two facets; therefore, without further insertion loss, a single laser can feed two of these structures and, with that, have two sensors. Two sensors may be arranged to have a differential and an offset measurement of the chip temperature if placing one structure close and another far for the active components. When the two gratings are subject to temperature, the two wavelengths shift and the shape changes, resulting in an interesting behavior. The next section illustrates the experimental setup and methodology used for the measurements.

3. Methodology and Experimental Setup

Figure 3 shows the schematic of the experimental setup of the test chip and the mapping of the PIC chip with the picture. In the presented case, and for the sake of temperature independence, a tunable LD was used for common mode.

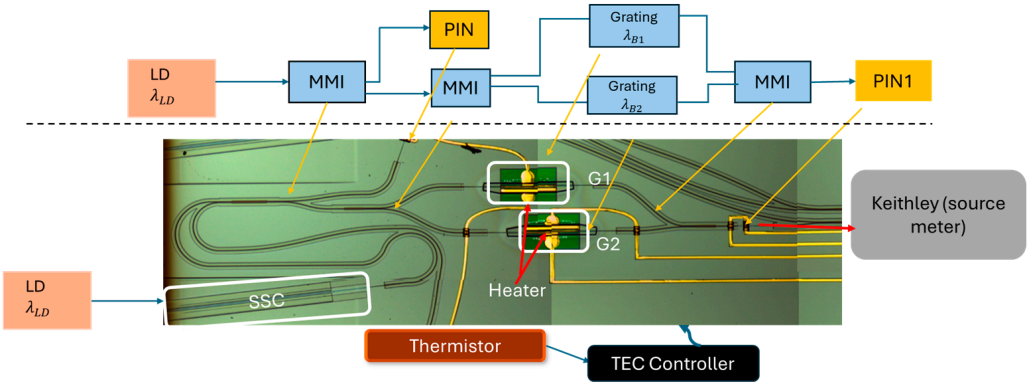

Figure 3. Testing assembly and experimental setup for the test chip, featuring physical integration with the InP chip for common mode testing and characterization.

PIN1 is used for monitoring the power that was arriving to the chip. The temperature of the chip was changed through a commercial TEC controller that measured the temperature with a calibrated thermistor. With this setup, the wavelength of the LD was changed from 1521 nm to 1530 nm to characterize the full range where the gratings were designed.

In the case of differential mode, the chip has G1 very close to the heating source. The next section provides the experimental results of the test chip.

4. Results and Discussion

The temperature of the chip was varied (19 °C to 45 °C) by changing the parameters at the TEC controller.

The optical power, P, is estimated from the measurements in the current of the PIN1 for several temperatures in accordance with Figure 4. PIN1 is used to monitor power transmitted, which is obtained by the measured voltage and converted as in Equation (1).

$$\mathrm{P(dBm)} = 10log_{10}\left(\frac{1000 \times \mathrm{V(Volt)}}{\mathrm{R}(\Omega) \times \mathrm{R_{PIN}}\left(\frac{\mathrm{A}}{\mathrm{W}}\right)}\right), \quad (1)$$

where 'V' is the voltage measured across the PINs, 'R' is the resistor for the current conversion (10 KΩ), and 'R_{PIN}' is the PIN responsivity.

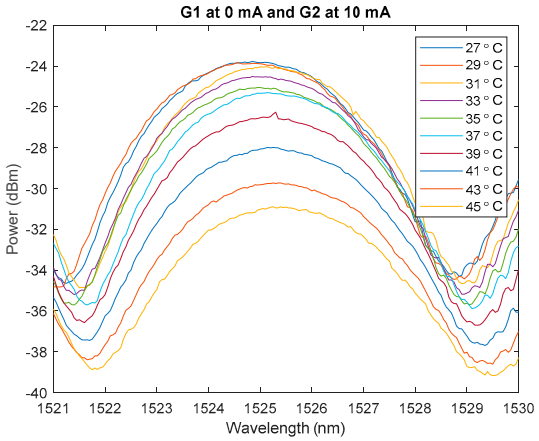

Figure 4. Transmission signal as a function of the wavelength for different TEC temperatures.

In Figure 4 the behavior of the structure is presented for the overlapping section of the response, showing an interesting behavior in the range from 1524 nm up to 1526.5 nm with LD to be 2.5 nm with a measurement error of less than 0.5 dB, which corresponds to less than 0.17 dB/°C. The region is important as it clearly demonstrates the impact of temperature on power. In Figure 5, a detail of the behavior in the most favorable range is presented (the slope behavior is negative due to the impact of lower Bragg wavelength, i.e., 1522 nm is closer to the heat source with more impact of heating compared to negligible impact Bragg wavelength 1529 nm). The sensitivities at 1524 nm, 1525 nm, and 1526 nm are 1.45 dB/°C, 1.62 dB/°C, and 1.6 dB/°C, respectively, for differential mode. Similarly, for common mode, the behavior in the most favorable is illustrated in Figure 6. The sensitivity noted for this case is 0.8 dB/°C at 1524 nm.

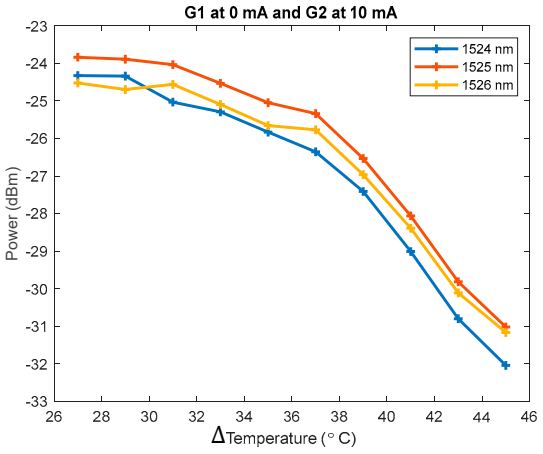

Figure 5. Power vs. temperature observed at wavelengths of 1524 nm, 1525 nm, and 1526 nm from 26 °C to 46 °C for differential mode.

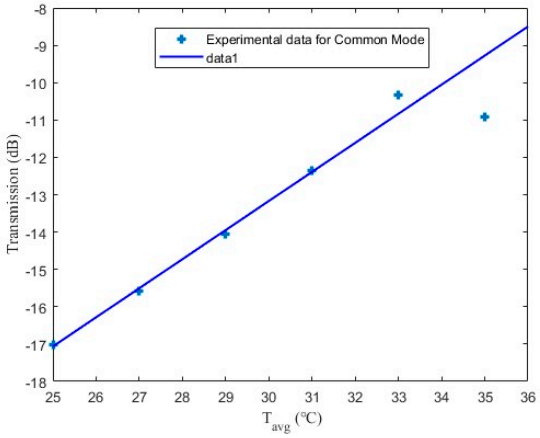

Figure 6. Common mode transmission signal vs. temperature response at 1524 nm.

5. Conclusions

This work provides concrete experimental evidence of the possibility to detect the relative temperature using differential mode, also an extension of the previous work [9] regarding temperature monitoring on the surface of the chip. The structure is potentially very small and can be replicated, without major impact, along the chip, allowing local thermal monitoring. This approach grants improvement in the quality of the chip performance, therefore with potential impact in the increased chip yield. Theoretically, power sensitivity was observed to be 0.77 dB/°C and 0.98 dB/°C for common mode and differential mode, respectively. The experimentally noted sensitivity of common mode and differential mode are 1.45 dB/°C and 0.8 dB/°C, respectively, at 1524 nm.

Author Contributions: Conceptualization, S.P. and A.T.; methodology, S.P.; software, S.P.; validation, S.P., A.T. and M.L.; formal analysis, S.P.; investigation, S.P.; resources, A.T. and M.L.; data curation, S.P.; writing—original draft Preparation, S.P.; writing—review and editing, S.P., A.T. and M.L.; visualization, S.P.; supervision, A.T. and M.L.; project administration, A.T. and M.L.; funding acquisition, S.P. and A.T. All authors have read and agreed to the published version of the manuscript.

Funding: This work was supported by the project PLUGPON (POCI-01-0247-FEDER-047221), FCT PhD grant 2021. 05090.BD.

Institutional Review Board Statement: Not applicable.

Informed Consent Statement: Not applicable.

Data Availability Statement: It is present in Section 4.

Conflicts of Interest: The authors declare no conflict of interest.

References

1. Butt, M.A.; Kazanskiy, N.L.; Khonina, S.N. Advances in Waveguide Bragg Grating Structures, Platforms, and Applications: An Up-to-Date Appraisal. *Biosensors* **2022**, *12*, 497. [CrossRef] [PubMed]
2. Carpintero, G.; Hisatake, S.; de Felipe, D.; Guzman, R.; Nagatsuma, T.; Keil, N. Wireless Data Transmission at Terahertz Carrier Waves Generated from a Hybrid InP-Polymer Dual Tunable DBR Laser Photonic Integrated Circuit. *Sci. Rep.* **2018**, *8*, 3018. [CrossRef] [PubMed]
3. Gilardi, G.; Yao, W.; Haghighi, H.R.; Smit, M.K.; Wale, M.J. Substrate Thickness Effects on Thermal Crosstalk in InP-Based Photonic Integrated Circuits. *J. Light. Technol.* **2014**, *32*, 3061–3066. [CrossRef]
4. Pandey, S.; Pinho, C.M.R.; Rodrigues, F.; Neto, H.; Lima, M.; Teixeira, A.L.J. Laser Thermal Crosstalk Modelling in InP based Photonic Integrated Chips. In Proceedings of the 2019 SBMO/IEEE MTT-S International Microwave and Optoelectronics Conference (IMOC), Aveiro, Portugal, 10–14 November 2019; pp. 1–3.
5. Mathews, I.; Abdullaev, A.; Lei, S.; Enright, R.; Wallace, M.J.; Donegan, J.F. Reducing thermal crosstalk in ten-channel tunable slotted-laser arrays. *Opt. Express* **2015**, *23*, 23380–23393. [CrossRef] [PubMed]

6. Gilardi, G.; Yao, W.; Smit, M.K.; Wale, M.J. On-Chip Thermal Crosstalk Reduction in InP-based Photonic Integrated Circuits. In *Advanced Photonics for Communications*; OSA Technical Digest (online); Optica Publishing Group: Washington, DC, USA, 2014; paper IM3A.1.
7. Carroll, L.; Lee, J.S.; Scarcella, C.; Gradkowski, K.; Duperron, M.; Lu, H.; Zhao, Y.; Eason, C.; Morrissey, P.; Rensing, M.; et al. Photonic packaging: Transforming silicon photonic integrated circuits into photonic devices. *Appl. Sci.* **2016**, *6*, 426. [CrossRef]
8. Klimov, N.N.; Mittal, S.; Berger, M.; Ahmed, Z. On-chip silicon waveguide Bragg grating photonic temperature sensor. *Opt. Lett.* **2015**, *40*, 3934–3936. [CrossRef] [PubMed]
9. Pandey, S.; Abejide, A.E.; Rodrigues, F.; Lima, M.; Teixeira, A. Grating-Based Structure for in-PIC Temperature Monitoring. In Proceedings of the 2023 23rd International Conference on Transparent Optical Networks (ICTON), Bucharest, Romania, 2–6 July 2023; pp. 1–4.